Proc. Indian Acad. Sci. (Chem. Sci.), Vol. 110, No. 3, June 1998, pp. 277–295.

Interfacial electron transfer from nonstoichiometric cadmium sulfide nanoparticles to free and complexed copper(II) ions in 2-propanol

ALEX V ISAROV and JOHN CHRYSOCHOOS*
Department of Chemistry, The University of Toledo, Toledo, Ohio 43606, USA

Abstract. The interactions of free and complexed copper ions ($Cu(ClO_4)_2$, $Cu(acac)_2$, and CuTPP) with the surface of nonstoichiometric CdS nanoparticles were monitored by EPR spectroscopy, recombination luminescence quenching and UV/VIS absorption spectroscopy. It was found that formation of a surface S–Cu bond takes place both in the case of $Cu(ClO_4)_2$ (free Cu^{2+} ions) and $Cu(acac)_2$. This process is accompanied by thermal (dark) reduction of Cu^{2+} to Cu^{+}, formation of a new energy level in the semiconductor bandgap and quenching of the original recombination luminescence of the nanoparticles. The quenching data obey a static interaction model, which confirms binding of copper ions onto the surface of CdS nanoparticles. In addition, $Cu(acac)_2$ molecules can interact with Cd^{2+} ions on the surface of CdS, leading to a less effective quenching of the recombination luminescence of CdS, compared to that by free copper ions. In contrast to the behavior of $Cu(ClO_4)_2$ and $Cu(acac)_2$, copper(II) tetraphenylporphyrin does not interact directly with the surface of CdS nanoparticles, leading to a very negligible quenching of the recombination luminescence of CdS (e_{tr}^-/h_{tr}^+) nanoparticles.

Keywords. Complexed copper ions; recombination luminescence; EPR spectroscopy.

1. Introduction

Colloidal semiconductor nanoparticles are widely used for the investigation of photo-induced interfacial electron transfer [1–6]. The surface of the nanoparticles plays a very important role in this process [1,c,d]. Therefore, surface modification of semiconductor nanoparticles by adsorption of various molecules and ions can change their optical, chemical and photocatalytic properties significantly [7–19]. Adsorbed molecules and ions can form surface electron traps whose electronic energy may be lower than the energy of the electron in the conduction band of the semiconductor nanoparticle (E_e). The latter is dependent upon the size of the nanoparticles [20]

$$E_e = E_g + (\hbar^2\pi^2/2R^2)(1/m_e^* + 1/m_h^*) - 1{\cdot}8e^2/\varepsilon R + \text{polarization terms}$$

where E_g is band gap energy of the bulk semiconductor, m_e^* and m_h^* the effective masses of the electron and hole, respectively, and R the radius of the nanoparticle.

In the particular case of metal chalcogenides, surface modification can be attained by the adsorption of metal ions (free and complexed) onto the nanoparticle surface [7–14,16–19,21]. Therefore, the interactions of adsorbed metal ions, free and complexed, with semiconductor nanoparticles need to be studied thoroughly to elucidate interfacial electron transfer.

*For correspondence

The dynamics of interfacial electron transfer reactions, which represent the primary step of photocatalytic action by semiconductor nanoparticles, are being studied in terms of both the redox potential of the electron donor and the electron acceptor and in terms of surface adsorbate-adsorbent interactions [1c,d]. In the case of adsorbed metal complexes the electron transfer mechanism depends upon the chemical properties of both the metal and the ligand (coordination environment). For example, interactions of CdS nanoparticles with free trivalent lanthanide ions led to quenching of the recombination luminescence of CdS (e_{tr}^-/h_{tr}^+) nanoparticles with an efficiency which was found to be dependent upon the redox potential of the ion, $E^0(Ln^{3+}/Ln^{2+})$ [2,3]. On the other hand, interactions of CdS nanoparticles with lanthanide β-diketonate complexes ($Ln(fod)_3$) led to an antiquenching effect [21a], namely luminescence enhancement. In contrast to the quenching effect of Ln^{3+}-ions, the relative quenching efficiency of the recombination luminescence of CdS (e_{tr}^-/h_{tr}^+) nanoparticles by metalloporphyrins (MTPP, M = Mg, Zn, Cd, Cu, Co and Ni) does not follow the trend of the redox potential of MTPP [6]. One can assume that this observation indicates the different ability of metalloporphyrins to adsorb onto the surface of CdS nanoparticles. In addition, interactions of ferrocene derivatives with the surface of CdS nanoparticles were found to be highly dependent on the nature of the functional groups present in ferrocene [21b].

Surface modification of II–VI semiconductor nanoparticles with free metal ions leads to either isolated adsorbed metal ions or formation of ultrasmall particles of corresponding metal chalcogenides [7a,c,9–14,22]. Several metal ions have been investigated from the point of view of their interactions with the surface of semiconductor nanoparticles: Mn [9], Ag[10,19], Zn, Cd, Hg, and Pb (see [7c] and references therein). We reported earlier the formation of isolated Cu^+ ions and particles of Cu_2S onto the surface of nonstoichiometric CdS nanoparticles after the addition of $Cu(ClO_4)_2$ [22]. It is well known that the reaction of copper(II) chelates with S^{2-}, for the synthesis of bulk copper sulfide, leads to the formation of an unusual metastable form of the latter [23]. Therefore, one may also expect that the use of stable copper(II) chelate compounds for surface modification of nonstoichiometric CdS nanoparticles would lead to the formation of nanoparticles with unusual and interesting properties.

The present work is designed to investigate the effect of the coordination of Cu^{2+} ions (free, complexed) on their interactions with nonstoichiometric cadmium sulfide nanoparticles. Electron transfer reactions (thermal and light-induced) were monitored by EPR, which is linked to the reduction of Cu^{2+} ($3d^9$) to Cu^+ ($3d^{10}$) ions, and by quenching of the recombination luminescence of CdS nanoparticles. Copper(II) acetylacetonate and copper(II) tetraphenylporphyrin (CuTPP) were used as complexed copper compounds. The results obtained with $Cu(acac)_2$ and CuTPP will be presented in comparison with the results reported earlier for free Cu^{2+} ions [22]. A few experiments on the interaction of $Cu(acac)_2$ and CuTPP with sulfide ions and cadmium ions in 2-propanol were also carried out to explore the role of S^{2-}- and Cd^{2+}-surface ions in CdS nanoparticles.

2. Experimental

Cadmium sulfide nanoparticles were prepared in 2-propanol at − 78°C without added stabilizers, using well established literature techniques of "arrested precipitation" [24]. The preparation was carried out by a rapid mixing of a solution of $1{\cdot}2 \times 10^{-3}$ M

$Cd(ClO_4)_2 \cdot 6H_2O$ in 2-propanol with a freshly prepared solution of Na_2S in a mixture of 2-propanol-methanol (6:1) in the presence of an excess of NaOH. Both solutions were precooled and deaerated before mixing. Semiconductor nanoparticles prepared in this way had a $[Cd^{2+}]/[S^{2-}]$-ratio equal to 3 (nonstoichiometric CdS nanoparticles); they were stabilized against precipitation by their electrostatic double layer repulsion [24]. Such nanoparticles remained stable for at least a month at 0°C.

The optical band gap energy of CdS nanoparticles (E_g) was calculated via the absorption coefficient of the edge-to-edge absorption band, $\alpha(h\nu)$, associated to direct transitions in CdS ($k = 0 \rightarrow k = 0$) [25,26],

$$\alpha(h\nu) = \{e^2(2m_h^* m_e^*/(m_h^* + m_e^*))^{3/2}/nch^2 m_e^*\}(h\nu - E_g)^{1/2},$$

where m_h^* and m_e^* are the effective masses of the hole and the electron, respectively. E_g values were found to be about 3·05 eV (ranging from 3·0 eV to 3·1 eV for different preparations) from the straight lines of $\{\alpha(h\nu)\}^2$ vs $h\nu(eV)$, as $\alpha(h\nu) \rightarrow 0$.

The addition of free Cu^{2+} ions to the colloidal solution of CdS nanoparticles was carried out in the form of 1×10^{-3} M solution of $Cu(ClO_4)_2 \cdot 6H_2O$ in 2-propanol. Copper(II) acetylacetonate and copper(II) tetraphenylporphyrin are not readily soluble in 2-propanol. Therefore, 1×10^{-3} M solution of $Cu(acac)_2$ in methanol or 1×10^{-3} M solution of CuTPP in chloroform were used instead. The resulting change in the composition of the solvent (in the absence of the corresponding copper compound) did not affect the optical properties of CdS nanoparticles.

Ultraviolet and visible absorption spectra were recorded with a Hewlett-Packard 8452A Diode Array spectrophotometer. Luminescence spectra were recorded with an Aminco-Bowman spectrophotofluorimeter. EPR spectra were recorded using a Bruker ESP 300 E spectrometer.

Copper tetraphenylporphyrin was synthesized from purified H_2 TPP (chlorin free) [27] and copper acetate, using standard literature preparation and chromatographic purification methods [28]. All other chemicals used were of the highest purity available commercially.

3. Results

3.1 *Absorption and emission spectra*

Figure 1 shows the absorption spectra of nonstoichiometric CdS nanoparticles (2×10^{-4} M) in the presence of added $Cu(ClO_4)_2$ (A) and $Cu(acac)_2$ (B), ranging from 3×10^{-6} M to 1×10^{-4} M. Spectra were recorded 1 hour after preparation.

In the presence of copper(II) perchlorate, the absorption spectrum of CdS nanoparticles becomes broader and the absorption edge shifts to longer wavelengths (figure 1A), as it was reported earlier [22]. The negligible absorptivity of CdS nanoparticles at $\lambda > 450$ nm increases considerably in the presence of $Cu(ClO_4)_2$. On the other hand, addition of copper(II) acetylacetonate to CdS nanoparticles in 2-propanol did not affect the absorption spectrum of CdS (figure 1B), in contrast to the effect described in figure 1A. A slight increase of the absorptivity observed below 360 nm is attributed to the absorptivity of the acetylacetonate ligand itself ($\lambda_{max} = 294$ nm). No increase in the absorptivity was observed at longer wavelengths. The absorption spectra of CdS nanoparticles in the presence of CuTPP do not exhibit any significant changes other than that expected due to the absorption of CuTPP itself.

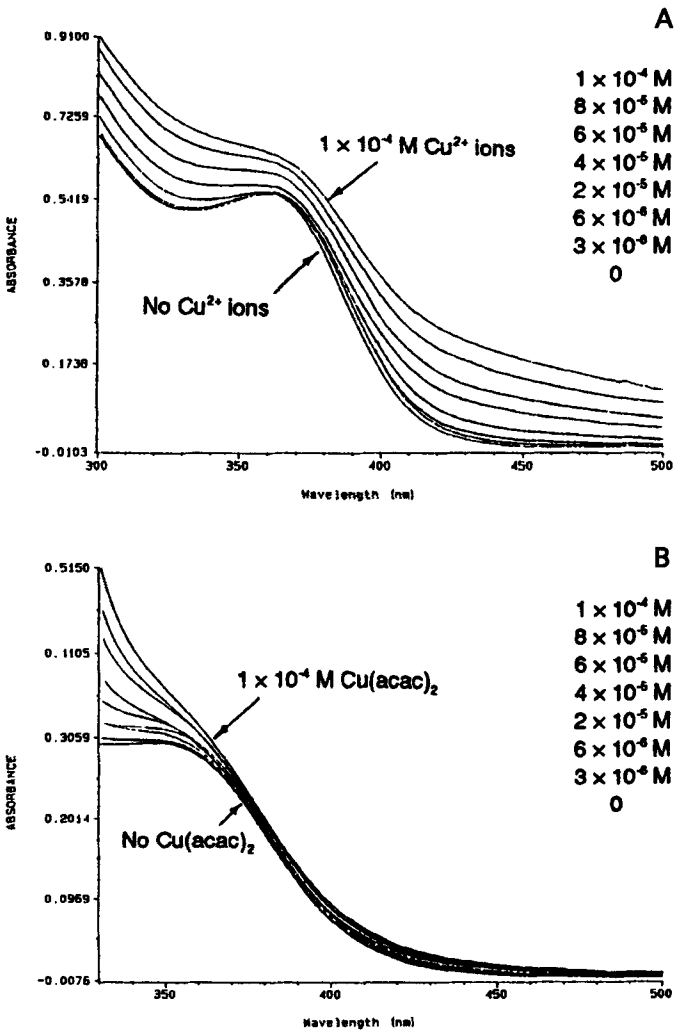

Figure 1. Absorption spectra of nonstoichiometric CdS nanoparticles (2×10^{-4} M CdS, 4×10^{-4} M excess Cd^{2+} and 2×10^{-4} M NaOH in 2-propanol) in the absence and presence of various amount of (**A**): $Cu(ClO_4)_2$ and (**B**): $Cu(acac)_2$ (as indicated). Part A-reprinted from ref. 22. (Copyright 1996 American Chemical Society).

Although the absorption spectrum of CdS nanoparticles is mostly unaffected by the addition of copper(II) acetylacetonate, the defect recombination luminescence of CdS (e_{tr}^-/h_{tr}^+) nanoparticles ($\nu_{max} = 17900\,cm^{-1}$) is quenched in the presence of copper(II) acetylacetonate (figure 2). The luminescence quenching is accompanied by a gradual red shift of the emission maximum. This observation implies the formation, as in the case of copper(II) perchlorate [22], of a red-shifted component in the emission spectra. However, addition of CuTPP to CdS nanoparticles, under identical conditions, had a very minor effect upon the recombination luminescence spectra of CdS (e_{tr}^-/h_{tr}^+) nanoparticles (corrected for the absorption of CuTPP itself).

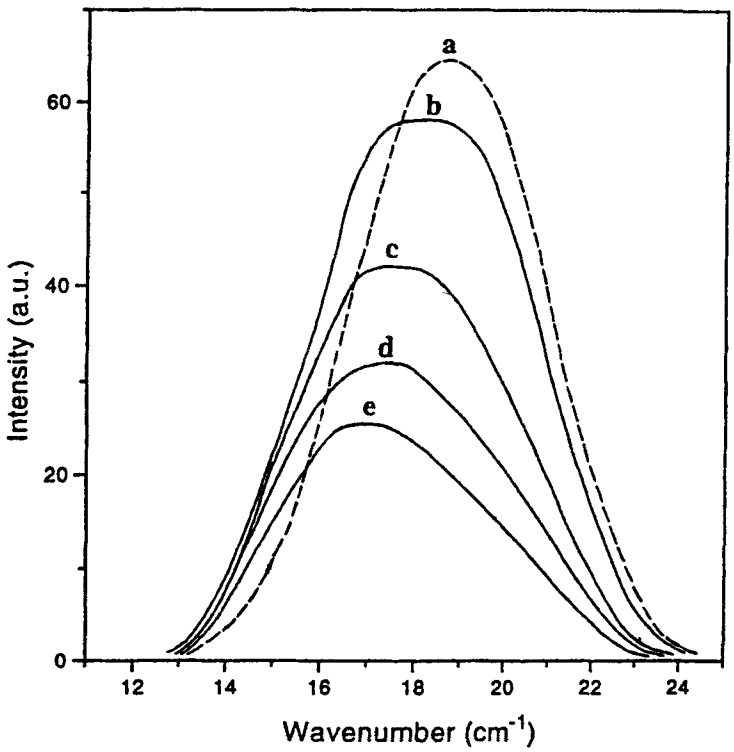

Figure 2. Recombination luminescence spectra of 2×10^{-4} M nonstoichiometric CdS nanoparticles in 2-propanol at the following $Cu(acac)_2$ concentrations: (**a**) 0 M, (**b**) 1×10^{-6} M, (**c**) 2×10^{-6} M, (**d**) 4×10^{-6} M and (**e**) 1×10^{-5} M. The excitation wavelength was at 360 nm.

3.2 *Analysis of the emission spectra*

The analysis of the spectral distribution in the recombination luminescence spectra of nonstoichiometric CdS nanoparticles in the presence of free Cu^{2+} ions was carried out using a computer deconvolution technique, as reported earlier [22]. The same computer-based deconvolution technique was applied in this work for the analysis of the recombination luminescence spectrum of CdS nanoparticles in the presence of $Cu(acac)_2$. It was assumed that the emission spectrum of CdS nanoparticles in the presence of 1×10^{-6} M of $Cu(acac)_2$ is a superposition of the original emission band ($\nu_{max} = 17900\,cm^{-1}$, $\Delta\nu_{1/2} = 4500\,cm^{-1}$) and a new band which needs to the determined. As we reported earlier [22], the recombination luminescence spectrum of non-stoichiometric CdS nanoparticles (corrected for the photomultiplier tube response) fits a Gaussian line shape (figure 3).

The result of the deconvolution of the emission spectra of CdS nanoparticles in the presence of 1×10^{-6} M $Cu(acac)_2$, corrected for the photomultiplier tube response, is presented in figure 4. The contribution of the original emission band ($\nu_{max} = 17900\,cm^{-1}$) to the spectrum under consideration was determined by adjusting the height of the former to obtain the best possible fit of the high energy portion of the spectrum (figure 4). The second band ($\nu_{max} = 15100\,cm^{-1}$, $\Delta\nu_{1/2} = 3700\,cm^{-1}$), which

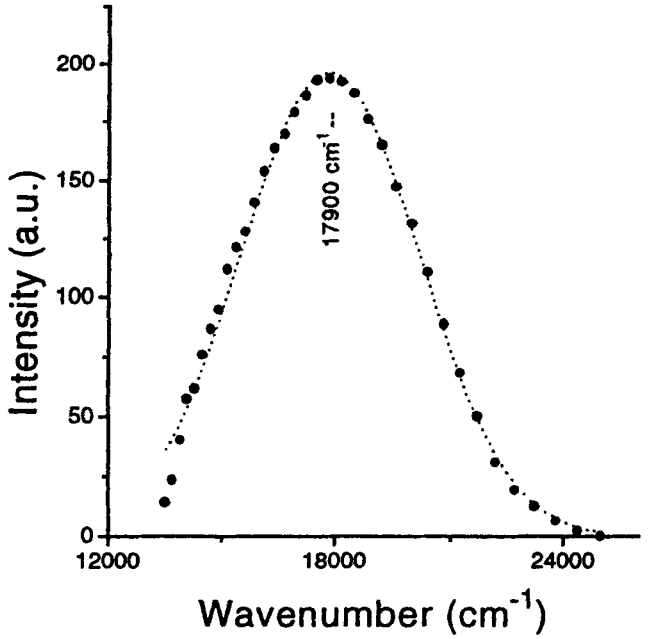

Figure 3. Recombination luminescence spectrum of 2×10^{-4} M nonstoichiometric CdS nanoparticles in 2-propanol ($\lambda_{exc} = 360$ nm). The points represent experimental data, corrected for the photomultiplier tube response; the dotted line represents a computer Gaussian line shape fit. Reprinted from ref 22. (Copyright 1996 American Chemical Soceity).

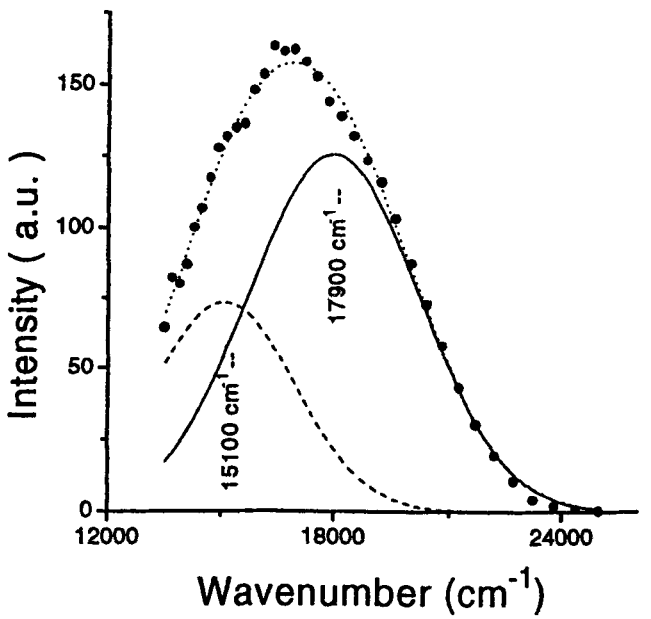

Figure 4. Deconvolution of the recombination luminescence spectrum of 2×10^{-4} M nonstoichiometric CdS nanoparticles in the presence of 1×10^{-6} M of $Cu(acac)_2$. The points represent experimental data, corrected for the photomultiplier tube response. The solid line represents a Gaussian line shape fit to the emission of CdS nanoparticles (first component). The dashed line represents the Gaussian line shape fit to the difference between the experimental spectrum and the first component. The dotted line represents the sum of the two Gaussian line shapes.

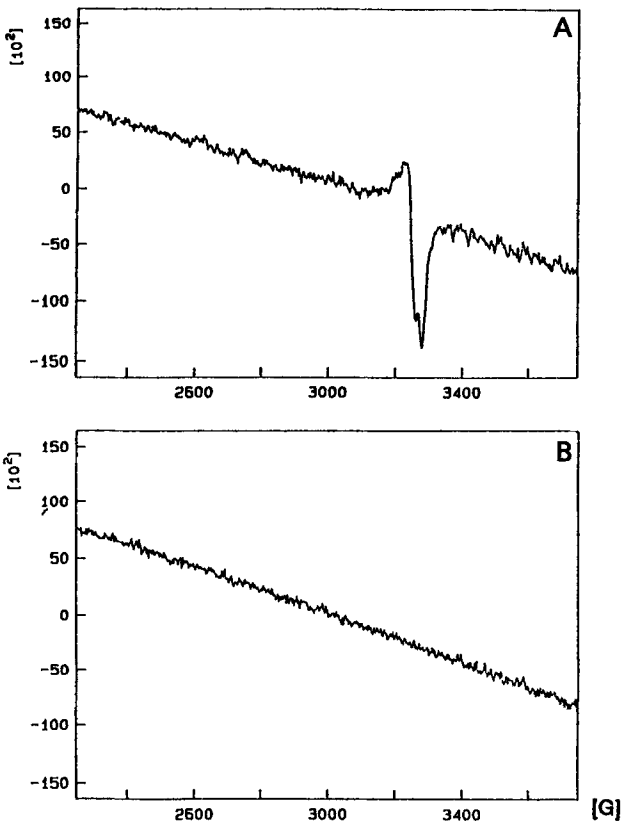

Figure 5. EPR spectra of 1×10^{-4} M $Cu(ClO_4)_2$ in 2-propanol in the absence (A) and in the presence (B) of 2×10^{-4} M of nonstoichiometric CdS nanoparticles. Spectra were recorded at 77 K.

also fits a Gaussian line shape (dashed line), was obtained by subtracting the computer generated Gaussian line shape of the first component from the experimental emission band. The sum of the two Gaussian components (dotted spectrum) is in a close agreement with the experimental emission spectrum (figure 4).

The position of the new red-shifted band, which appears in the emission spectra of CdS in the presence of copper(II) acetylacetonate ($\nu_{max} = 15100\,cm^{-1}$) is very close to that which was found in the spectrum of CdS nanoparticles in the presence of copper(II) perchlorate ($\nu_{max} = 14700\,cm^{-1}$) [22]. One can assume that both new emission bands have a similar origin.

3.3 *Electron paramagnetic resonance spectra*

The influence of nonstoichiometric CdS nanoparticles on the oxidation state of free copper ions has been studied earlier by EPR spectroscopy [22]. It was found that the addition of CdS nanoparticles to a solution of copper(II) perchlorate in 2-propanol led to the reduction of Cu^{2+} ions. At concentrations less than 5×10^{-5} M of $Cu(ClO_4)_2$ a complete reduction was observed after the addition of 2×10^{-4} M of CdS nanoparticles [22]. The same effect was observed at higher free Cu^{2+} ions concentration, namely 1×10^{-4} M of $Cu(ClO_4)_2$ (figure 5). The latter concentration of $Cu(ClO_4)_2$ is similar to

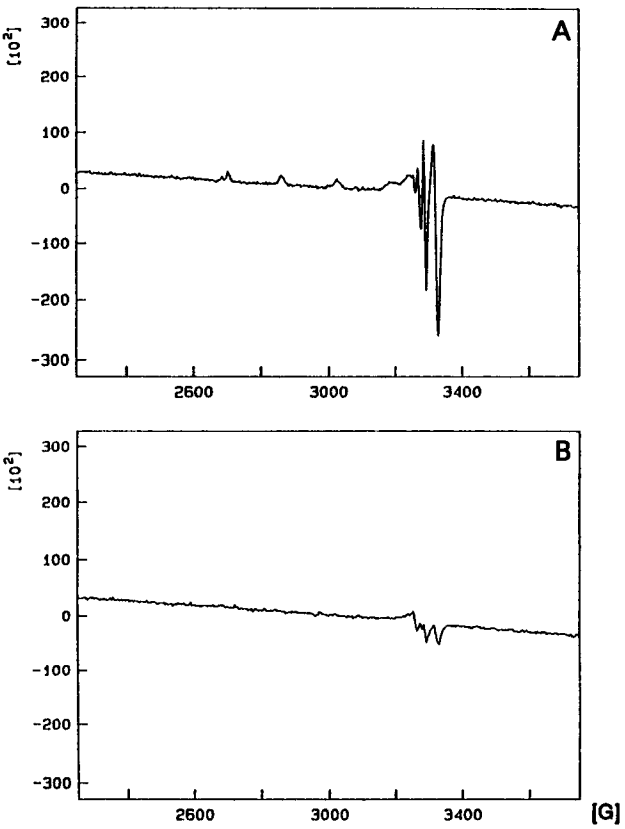

Figure 6. EPR spectra of 1×10^{-4} M $Cu(acac)_2$ in 2-propanol in the absence (A) and in the presence (B) of 2×10^{-4} M of nonstoichiometric CdS nanoparticles. Spectra were recorded at 77 K.

that of $Cu(acac)_2$ used in the experiments described in this paper. The perpendicular part of the EPR spectra of $Cu(ClO_4)_2$ disappears completely in the presence of 2×10^{-4} M of CdS nanoparticles. The parallel part of the EPR spectra is extremely weak and very poorly resolved.

Figure 6A shows the low temperature EPR spectrum of 1×10^{-4} M $Cu(acac)_2$ in 2-propanol-methanol solution (10% of methanol). This spectrum consists of two groups of four well resolved hyperfine lines (perpendicular and parallel regions) and it is very close to that described in the literature [29]. Addition of 2×10^{-4} M of CdS nanoparticles leads to a drastic decrease of the intensity of the EPR signal of $Cu(acac)_2$ (figure 6B). The spectra depicted on figure 6 were recorded 1 hour after the preparation of the samples.

The observations described in figures 6A and 6B imply the reduction of Cu^{2+} ions to Cu^{+} by CdS nanoparticles. It should be noted that the remaining relatively weak EPR signal in the perpendicular region (figure 6B) has a shape, which is different from the shape of the original spectrum. In a separate experiment, an EPR signal similar to that shown in figure 6B was assigned to a complex of $Cu(acac)_2$ with free Cd^{2+} ions in solution.

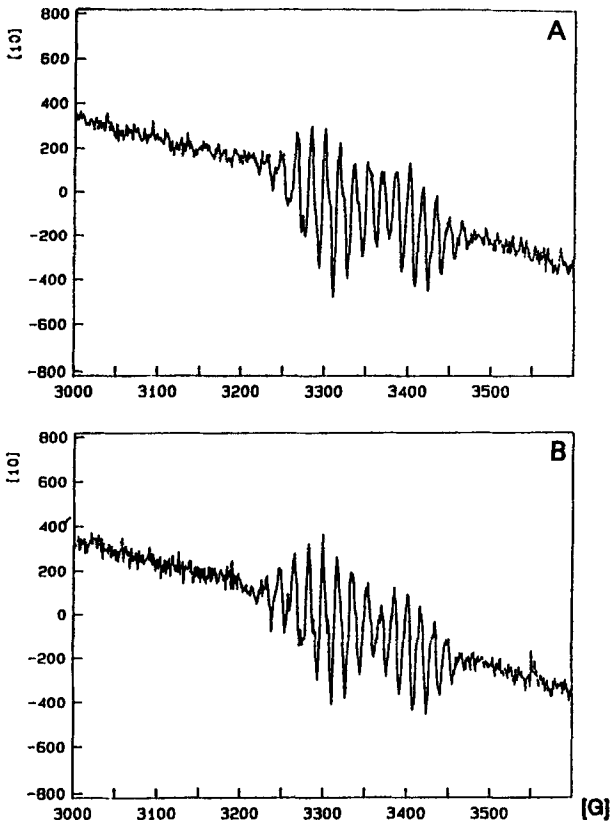

Figure 7. EPR spectra of 1×10^{-5} M CuTPP in 2-propanol in the absence (A) and in the presence (B) of 2×10^{-4} M of nonstoichiometric CdS nanoparticles. Spectra were recorded at 77 K.

Finally, the influence of CdS nanoparticles on the EPR spectra of copper(II) tetraphenylporphyrin has also been studied. Figure 7 shows low temperature (77 K) EPR spectra of 1×10^{-5} M of Cu(II)TPP (perpendicular region only) in a 2-propanol-chloroform solution (1% of chloroform) in the absence (A) and in the presence (B) of 2×10^{-4} M of CdS nanoparticles. The EPR spectrum of the frozen solution of Cu(II)TPP is very complex (figure 7A). Its perpendicular region consists of at least 18 overlapping lines corresponding to the hyperfine lines resulting from the interactions with both ^{63}Cu and ^{65}Cu isotopes, which are further split by superhyperfine interactions with the nitrogens of the pyrrole groups of a porphyrin ring. The detailed interpretation may be found elsewhere [30-32]. It is apparent that the EPR spectrum of CuTPP in the presence of 2×10^{-4} M of CdS nanoparticles (figure 7B) is identical to that in the absence of CdS (figure 7A). This means that the interactions of Cu(II)TPP with CdS nanoparticles have no effect upon either the oxidation state of copper, or its coordination environment.

3.4 *Time dependence of absorption spectra and the stability of CdS nanoparticles*

As we reported earlier [22], recombination luminescence, EPR and absorption spectra changed immediately after solutions of copper(II) perchlorate and nonstoichiometric

CdS nanoparticles were brought in contact. In the case of copper(II) acetylacetonate the situation is different. Whereas luminescence quenching and the formation of the red-shifted component resulted immediately following the addition of $Cu(acac)_2$ to CdS nanoparticles, UV/VIS spectra exhibit both immediate and gradual changes. The latter depend upon the concentration of the copper compound added.

Absorption spectra of CdS nanoparticles (stored at room temperature) in the presence of less than 1×10^{-5} M $Cu(acac)_2$ remain almost unchanged for several days. Under identical conditions of storage, the absorption spectra of pure CdS nanoparticles undergo gradual changes, namely the absorption edge shifts to shorter wavelengths. The latter effect indicates a gradual dissolution of CdS nanoparticles. Therefore, addition of low concentrations of $Cu(acac)_2$ (less than 1×10^{-5} M) appears to increase the stability of CdS nanoparticles stored at room temperature. No precipitation of these samples was observed even 20 days after preparation. A similar effect we observed earlier in the presence of copper(II) perchlorate [22].

On the other hand, at concentrations of $Cu(acac)_2$ higher than 1×10^{-5} M, the absorption spectra of CdS nanoparticles remain unchanged initially (several hours after preparation) and at longer time intervals they undergo very slow changes. The absorptivity at $\lambda > 450$ nm increases gradually, indicating formation of ultrasmall particles of Cu_2S on the surface of CdS nanoparticles [22]. Eventually, CdS nanoparticles precipitate. But the precipitation process, caused by the addition of $Cu(acac)_2$, is much slower than that caused by the addition of $Cu(ClO_4)_2$. For example, whereas 2×10^{-4} M of CdS nanoparticles containing 5×10^{-4} M of $Cu(ClO_4)_2$ precipitated in 2–3 h, the same concentration of CdS containing 5×10^{-4} M of $Cu(acac)_2$ did not precipitate 12 h after preparation. The last observation indicates that the reaction of CdS nanoparticles with $Cu(acac)_2$ occurs slowly compared to that with $Cu(ClO_4)_2$. Finally, the addition of Cu(II)TPP to the CdS nanoparticles did not change the stability of the latter. The absorption spectra of the mixture represent the sum of the spectra of the components (Cu(II)TPP and CdS nanoparticles), stored under identical conditions.

3.5 *Interaction of $Cu(acac)_2$ and CuTPP with S^{2-} and Cd^{2+} in 2-propanol*

To explore the interaction of $Cu(acac)_2$ and CuTPP with S^{2-} and Cd^{2+} ions on the surface of CdS nanoparticles, control reactions between $Cu(acac)_2$/CuTPP with S^{2-} and Cd^{2+} free ions in solution were monitored by UV/VIS spectroscopy and by EPR. Figure 8 shows the absorption spectra of 4×10^{-5} M of $Cu(acac)_2$ in 2-propanol-methanol (5% of methanol) in the absence (figure 8A) and in the presence (figure 8B) of 5×10^{-5} M S^{2-}. The absorption band at 244 nm disappears completely in the presence of S^{2-}. Simultaneously, the second absorption band (294 nm) increases almost twice in intensity and shifts to 296 nm. Since the absorption band at 244 nm in the spectrum of $Cu(acac)_2$ is attributed to charge transfer from the ligand to the metal [33], the disappearance of this band implies reduction of Cu^{2+} to Cu^{+} in the presence of S^{2-}. This assumption is confirmed by EPR spectroscopy. The EPR signal of 4×10^{-5} M $Cu(acac)_2$ (figure 9A) disappears completely after addition of 5×10^{-5} M sulfide ions (figure 9B). The appropriate EPR spectra show that the shape of the EPR signal of $Cu(acac)_2$ does not change with the addition of S^{2-}, but its intensity is reduced proportionally to $[S^{2-}]$.

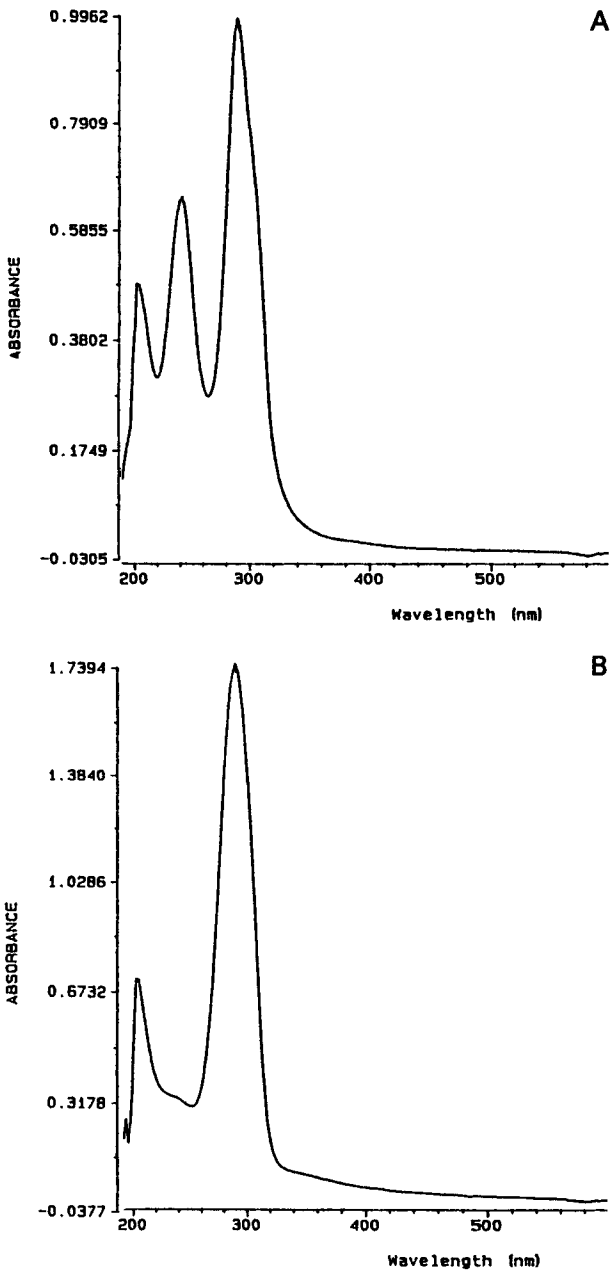

Figure 8. Absorption spectra of 4×10^{-5} M of $Cu(acac)_2$ in 2-propanol-methanol (5% of methanol) in the absence (A) and in the presence (B) of 5×10^{-5} M Na_2S in a mixture of 2-propanol-methanol (0·2% of methanol).

In addition, $Cu(acac)_2$ interacts also with Cd^{2+} ions in solution. Figure 10 shows the absorption spectra of 4×10^{-5} M of $Cu(acac)_2$ in 2-propanol-methanol (5% of methanol) in the absence (figure 10A) and in the presence (figure 10B) of 8×10^{-4} M of Cd^{2+}. The addition of Cd^{2+} ions leads to the reduction of the intensity of the

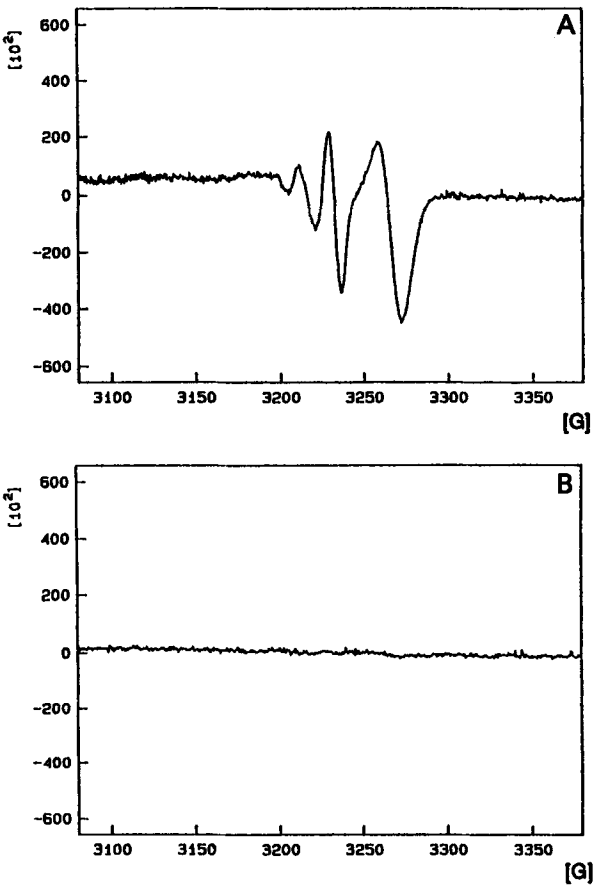

Figure 9. EPR spectra of 4×10^{-5} M $Cu(acac)_2$ in 2-propanol-methanol (5% of methanol) in the absence (**A**) and in the presence (**B**) of 5×10^{-5} M Na_2S in a mixture of 2-propanol-methanol (0·2% of methanol). Spectra were recorded at 77 K.

absorption band at 244 nm by about 50%, whereas the absorption band at 294 nm remains almost unchanged. Further increase of Cd^{2+} concentration does not change the absorption spectra. It is apparent that no reduction of Cu^{2+} to Cu^{+} is responsible for the reduction of the band at 244 nm in this case.

Addition of Cd^{2+} ions to a solution of $Cu(acac)_2$ affects also the low temperature EPR spectrum of the latter (figure 11). Well resolved hyperfine lines in the perpendicular region shown in figure 11A, become broader in the presence of Cd^{2+} ions (figure 11B) and the ratio of their intensities changes, indicating the proximity of Cd^{2+} ions to the $Cu(acac)_2$ molecule. One can assume a possible formation of a coordination bond between Cd^{2+} ion and delocalized π electrons or between Cd^{2+} ion and the oxygen atom of acetylacetonate ligand. The detailed analysis of these EPR spectra will be reported elsewhere.

Similar experiments were carried out with Cu(II)TPP replacing $Cu(acac)_2$. Addition of S^{2-} or Cd^{2+} had no effect upon either the absorption spectra or the EPR spectra of CuTPP.

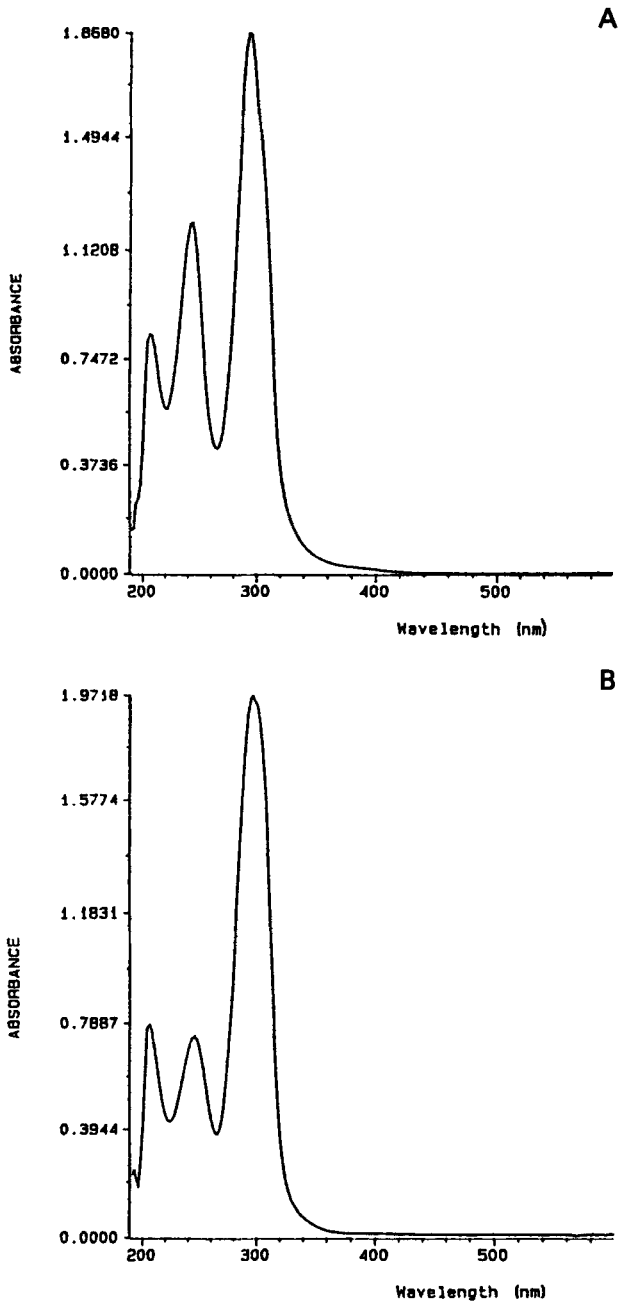

Figure 10. Absorption spectra of 4×10^{-5} M of $Cu(acac)_2$ in 2-propanol-methanol (5% of methanol) in the absence (**A**) and in the presence (**B**) of 8×10^{-4} M $Cd(ClO_4)_2$ in 2-propanol.

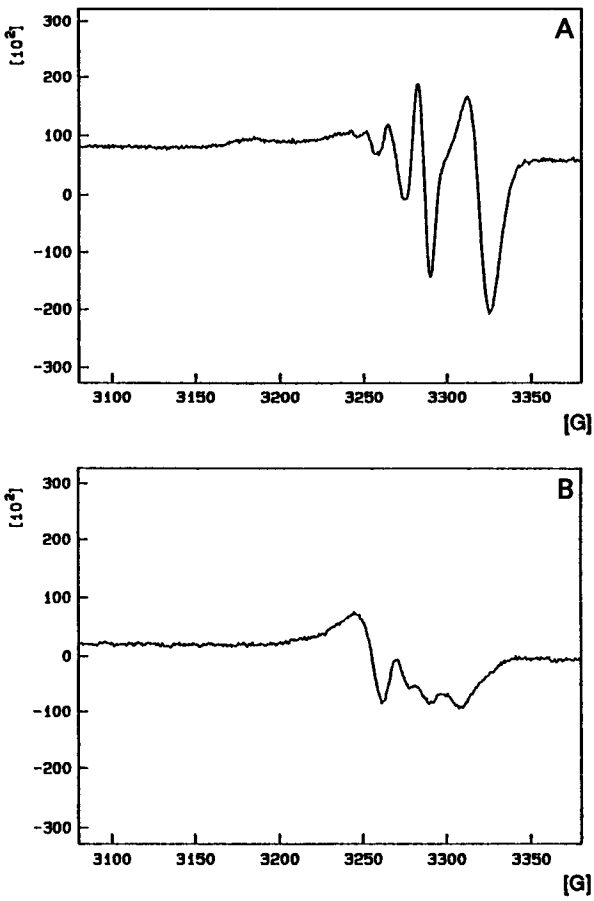

Figure 11. EPR spectra of 4×10^{-5} M of $Cu(acac)_2$ in 2-propanol-methanol (5% of methanol) in the absence (**A**) and in the presence (**B**) of 1×10^{-2} M $Cd(ClO_4)_2$ in 2-propanol. Spectra were recorded at 77 K.

Discussion

The effect of copper(II) acetylacetonate on the emission spectra of CdS nanoparticles consists of both, quenching of the original emission of nanoparticles (figure 2) and formation of new emission band at 15100 cm^{-1} (figure 4). This effect is very similar to that observed earlier for copper(II) perchlorate [22]. In the latter case the red-shifted emission band was assigned to a midgap energy level, located about 1·2 eV below conduction band, which was attributed to a surface S–Cu bond [34]. The appearance of the new red-shifted emission band in the case of $Cu(acac)_2$ is also evidence of formation of a S–Cu bond onto the surface of CdS.

Formation of a new midgap energy level facilitates electron-hole recombination [34,35], leading to the quenching of the original emission of nonstoichiometric CdS nanoparticles. The mathematical treatment of quenching data was carried out using a static interaction model between CdS nanoparticles and quencher [5,36,37]. According to this model,

$$I_F^Q = I_F^0 \exp(-K[Q]) \quad \text{or} \quad \ln(I_F^0/I_F^Q) = K[Q]$$

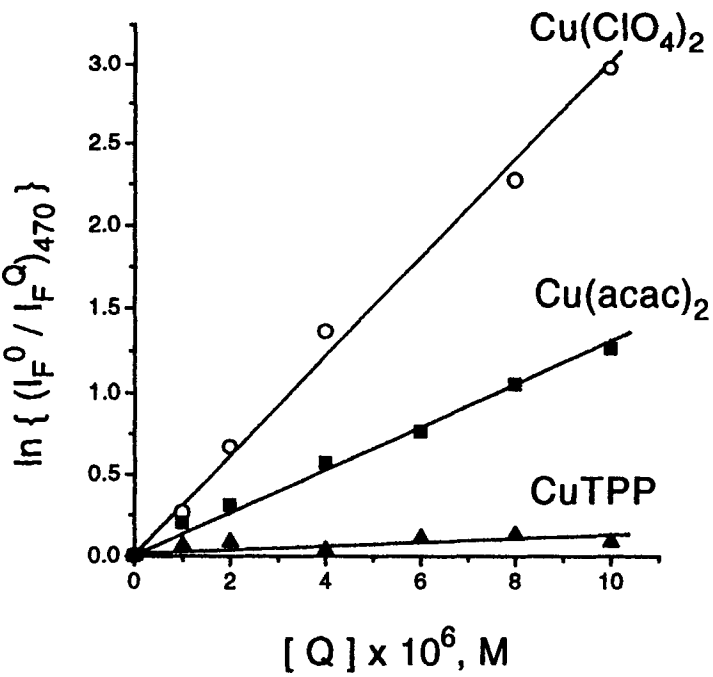

Figure 12. Semilogarithmic plots of (I_F^0/I_F^Q) of 2×10^{-4} M nonstoichiometric CdS nanoparticles *vs* the concentration of the appropriate copper compound (Q). Excitation wavelength at 360 nm. Emission wavelength at 470 nm.

where I_F^0 and I_F^Q are the intensities of the emission in the absence and presence of the quencher (Q) and K is the appropriate quenching constant. Figure 12 shows plots of ln (I_F^0/I_F^Q) *vs* the concentration of the copper compounds under consideration (Q). Data for free copper ions (copper(II) perchlorate) were taken from reference [22]. The fluorescence intensity (I_F) of CdS nanoparticles was monitored at 470 nm, where the contributions of new emission bands (14700 cm^{-1} and 15100 cm^{-1} for copper(II) perchlorate and copper(II) acetylacetonate respectively) are minimal. Fairly good straight line of $ln(I_F^0/I_F^Q)$ *vs* $[Q]$ obtained for the copper(II) acetylacetonate confirms the static interactions of $Cu(acac)_2$ molecules with CdS nanoparticles. The quenching of recombination luminescence of CdS nanoparticles by copper(II) acetylacetonate ($K = 1{\cdot}25 \times 10^5\ M^{-1}$), is less effective than that by copper(II) perchlorate ($K = 3{\cdot}0 \times 10^5\ M^{-1}$). Furthermore, the quenching of the recombination luminescence of the nonstoichiometric CdS nanoparticles by copper(II) tetraphenylporphyrin is very insignificant ($K < 1{\cdot}5 \times 10^4\ M^{-1}$).

The results of recombination luminescence quenching (figure 12) are in very good agreement with the results obtained by EPR (figures 5–7). Free copper(II) ions, which are most effective quenchers, get reduced completely in the presence of CdS nanoparticles (figure 5). Copper(II) tetraphenylporphyrin, whose EPR spectra do not undergo any change at all in the presence of nonstoichiometric CdS nanoparticles (figure 7), is the least effective quencher. Copper(II) acetylacetonate, which reveals intermediate quenching efficiency, undergoes incomplete reduction, accompanied by changes in the shape of its EPR spectra (figure 6).

As it was mentioned above, changes in the shape of EPR spectra of $Cu(acac)_2$ in the presence of CdS nanoparticles can be explained by the interaction of copper(II) acetylacetonate with cadmium ions in the solution. Therefore, there are at least two ways for copper(II) acetylacetonate to bind onto the surface of CdS nanoparticles.

(I) Direct formation of a S–Cu bond depicted schematically below

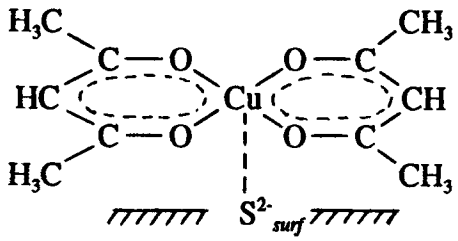

(A)

Formation of such a complex **A** on the surface of CdS nanoparticles leads to reduction of Cu^{2+} to Cu^{+}, which was observed by EPR (figure 6). This complex appears to be unstable and quickly loses one acetylacetonate ligand upon reduction,

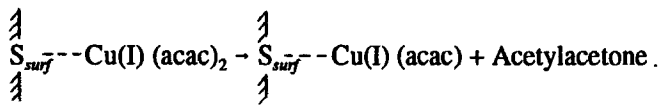

It is impossible to detect free acetylacetone molecules in the solution by UV/VIS absorption spectroscopy (band at 274 nm) because they instantly form complexes with free Cd^{2+} ions. This complex has a characteristic absorption band at 300 nm, which is masked by the absorption band of $Cu(acac)_2$ itself (294 nm).

Although the reaction of $Cu(acac)_2$ with the surface of CdS and the reduction of Cu^{2+} to Cu^{+} leads to the detachment of one acetylacetonate ligand, the remaining ligand is still bound to the adsorbed copper ion. As figure 1B demonstrates, addition of copper(II) acetylacetonate to nonstoichiometric CdS nanoparticles does not lead to the formation of ultrasmall particles of copper sulfide, at least in the early stages (absorption at $\lambda > 450$ nm belongs to copper sulfide, since bulk Cu_2S has a band gap energy $E_g = 1{\cdot}21$ eV [38]). One can assume that the remaining acetylacetonate ligand bound to Cu^{+} ion retards the formation of a copper(I) sulfide subphase.

(II) Adsorption of copper(II) acetylacetonate onto the surface of CdS nanoparticles which is not accompanied by the formation of S–Cu bond. The surface of

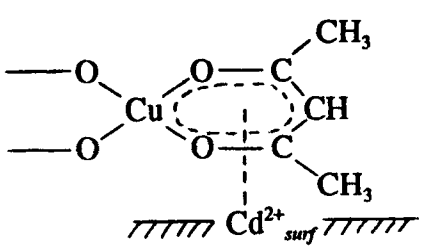

(B)

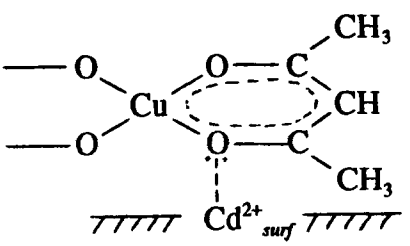

(C)

nonstoichiometric CdS nanoparticles, used in this work, is covered with a layer of adsorbed cadmium(II) ions. Therefore, the formation of complexes between adsorbed Cd^{2+} ions and delocalized π-electrons of the acetylacetonate ligand (B) or between adsorbed Cd^{2+} ions and free electron pairs of the ligand oxygen (C) is possible: Formation of these types of complexes does not lead to the immediate reduction of Cu^{2+} to Cu^{+}, as in the case of complex A. This assertion is supported by the EPR spectra shown in figure 6. The EPR signal of Cu^{2+} ions can be observed clearly one hour after the preparation of the sample.

Figure 13 shows the absorption spectra of 4×10^{-5} M $Cu(acac)_2$ (in propanol-methanol mixture) in the absence and presence of 2×10^{-4} M nonstoichiometric CdS nanoparticles. The latter was calculated by subtracting the spectrum of pure CdS nanoparticles from the spectrum of the mixture of CdS nanoparticles and corresponding amount of copper(II) acetylacetonate. The spectral changes caused by the addition of CdS nanoparticles consist of a slight red shift (3–4 nm) in the absorption band at 294 nm and the reduction of the intensity of the band at 244 nm by more than 50%. These spectral changes are very similar to those observed in solutions of $Cu(acac)_2$ (2-propanol) in the presence of free Cd^{2+} ions (figure 10) indicating that copper(II) acetylacetonate interacts with cadmium ions (free or surface-bound) in the presence of nonstoichiometric CdS nanoparticles.

It is very difficult to distinguish between complexes of Cd^{2+} ions with $Cu(acac)_2$ formed onto the surface of CdS nanoparticles or in the solution. The absorption spectra

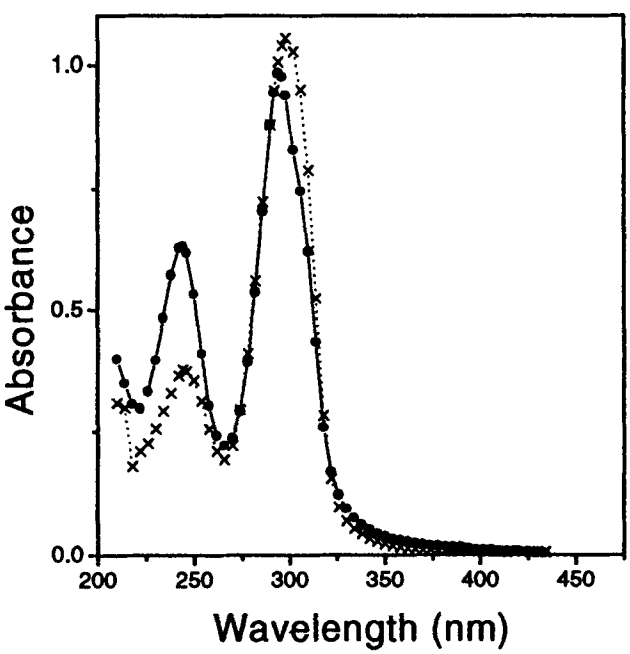

Figure 13. Absorption spectra of 4×10^{-5} M of $Cu(acac)_2$ in 2-propanol-methanol (5% of methanol) in the absence (dots) and in the presence (crosses) of 2×10^{-4} M nonstoichiometric CdS nanoparticles. The latter spectrum was calculated by subtracting the spectrum of pure CdS nanoparticles from the spectrum of the mixture of CdS nanoparticles and corresponding amount of copper(II) acetylacetonate.

of the mixture of copper(II) acetylacetonate and nonstoichiometric CdS nanoparticles (see section 3.4) change gradually with time, indicating the formation of the former complexes. The absorption spectra of samples containing more than 1×10^{-5} M of $Cu(acac)_2$ in the presence of CdS nanoparticles show a gradual increase of the absorptivity at $\lambda > 450$ nm, implying formation of ultrasmall particles of copper sulfide on the surface of nanoparticles. Eventually this process leads to the precipitation of the sample. At the same time the EPR signal of Cu^{2+} ions disappears completely. This means that the complex of Cd^{2+} with $Cu(acac)_2$ reacts gradually with CdS nanoparticles. This reaction requires adsorption of the complex onto the surface of the nanoparticles.

5. Conclusion

In this paper we have demonstrated the dependence of the interaction mechanism of copper(II) ions with the surface of nonstoichiometric CdS nanoparticles upon the structure of the ligand environment (coordination) of the ion. In the case of free copper(II) ions surface precipitation takes place [22]. Interaction of CdS nanoparticles with copper(II) acetylacetonate leads to the formation of quasi stable surface adducts, which eventually lose acetylacetonate ligands and form either isolated Cu^+ ions or ultrasmall particles of Cu_2S. The initial step of the interaction of $Cu(acac)_2$ with CdS nanoparticles consists of the formation of two types of surface complexes: complexes with S^{2-} and Cd^{2+} surface ions. Only the former complexes leads to the formation of a S–Cu bond and reduction of Cu^{2+} to Cu^+. This surface S–Cu bond creates a new energy level in the midgap, which is manifested in the formation of new band ($\nu_{max} = 15100\,cm^{-1}$) in the emission spectra of CdS nanoparticles.

Finally, copper(II) tetraphenylporphyrin does not react directly with the surface of CdS nanoparticles. The lack of the recombination luminescence quenching in this case is probably due to the weak adsorption of the porphyrin molecule onto the surface of cadmium sulfide.

References

1. For reviews, see: (a) Henglein A 1984 *Pure Appl. Chem.* **56** 1215 (b) Grätzel M 1989 *Heterogeneous photochemical electron transfer* (Boca Raton, Florida: CRC Press) p 87 (c) Kamat P V 1993 *Chem. Rev.* **93** 267 (d) Fox M A and Dulay M T 1993 *Chem. Rev.* **93** 341
2. Lee Y F, Olshavsky M and Chrysochoos J 1989 *J. Less-Common Met.* **148** 259
3. Chrysochoos J 1991 *J. Lumin.* **48&49** 709
4. Chrysochoos J 1991 *Mol. Cryst. Liq. Cryst.* **194** 247
5. Chrysochoos J 1992 *J. Phys. Chem.* **96** 2868
6. Bhamro and Chrysochoos J 1994 *J. Lumin.* **60&61** 359
7. For reviews, see: (a) Weller H 1993 *Angew. Chem., Int. Ed. Engl.* **32** 41 (b) Kamat P V 1993 *Chem. Rev.* **93** 267 (c) Weller H and Eychmüller A 1995 *Advances in Photochemistry* **20** 165 (d) Alivisatos A P 1996 *J. Phys. Chem.* **100** 13226 (e) Kamat P V 1997 *Prog. Inorg. Chem.* **44** 273
8. Spanhel L, Haase M, Weller H and Henglein A 1987 *J. Am. Chem. Soc.* **109** 5649
9. Sooklal K, Cullum B S, Angel S M and Murthy C J 1996 *J. Phys. Chem.* **100** 4551
10. Spanhel L, Weller H, Fojtik A and Henglein A 1987 *Ber. Bunsenges. Phys. Chem.* **91** 88
11. Hässelbarth A, Eychmüller A, Eichberger R, Giersig M, Mews A and Weller H 1993 *J. Phys. Chem.* **97** 5333
12. Weller H, Koch U, Gutiérrez M and Henglein A 1984 *Ber. Bunsenges. Phys. Chem.* **88** 649
13. Hoener C F, Allan K A, Bard A J, Campion A, Fox M A, Mallouk T E, Webber S E and White J M 1992 *J. Phys. Chem.* **96** 3812

14. (a) Zhou H S, Honma I, Komiyama H and Haus J W 1993 *J. Phys. Chem.* **97** 895
(b) Zhou H S, Sasahara H, Honma I, Komiyama H and Haus J W *Chem. Mater.* 1994 **6** 1534
15. Bedja I and Kamat P V *J. Phys. Chem.* 1995 **99** 9182
16. Tian Y, Newton T, Kotov N A, Guldi D M and Fendler J H *J. Phys. Chem.* 1996 **100** 8927
17. Mews A, Eychmüller A, Giersig M, Schooss D and Weller H 1994 *J. Phys. Chem.* **98** 934
18. Kamalov V F, Little R, Logunov S L and El-Sayed M A 1996 *J. Phys. Chem.* **100** 6381
19. Kumar A and Kumar S 1996 *Chem. Lett.* 711
20. Steigerwald M L and Brus L E 1990 *Acc. Chem. Res.* **23** 183
21. (a) Chandler R R and Coffer J L 1991 *J. Phys. Chem.* **95** 4 (b) Chandler R R, Coffer J L, Atherton S J and Snowden P T 1992 *J. Phys. Chem.* **96** 2713
22. Isarov A V and Chrysochoos J 1997 *Langmuir* **13** 3142
23. (a) Inoue M, Cruz-Vazquez C, Inoue M B and Fernando Q 1992 *J. Mater. Chem.* **2** 761 (b) Inoue M, Cruz-Vazquez C, Inoue M B, Nebesny K W and Fernando Q 1993 *Synth. Metals* **55–57** 3748 (c) Grijalva H, Inoue M, Boggavarapu S and Calvert P 1996 *J. Mater. Chem.* **6** 1157
24. Rossetti R, Hull R, Gibson J M and Brus L E 1985 *J. Chem. Phys.* **82** 552
25. Pankove J J 1971 In *Optical properties in semiconductors* (Englewood Cliffs, NJ: Prentice-Hall)
26. Wang Y, Suna A, Mahler W and Kasowski R 1987 *J. Chem. Phys.* **87** 7315
27. Barnett G H, Hudson M F and Smith K M 1973 *Tetrahedron Lett.* 2887
28. Adler A D, Longo F R, Kampas F and Kim J 1970 *J. Inorg. Nucl. Chem.* **32** 2443
29. Vänngard T 1972 In *Biological application of electron spin resonance* (eds) H M Swartz, J R Bolton, D C Borg (New-York: Wiley - Interscience) p 411
30. Lin W C 1979 In *The porphyrins* (ed.) D Dolphin (New York: Academic Press) vol. 4 chap. 7 p 355
31. Assour J M 1965 *J. Chem. Phys.* **43** 2477
32. Manoharan P T and Rogers M T 1969 In *Electron spin resonance of metal complexes* (ed.) T F Yen (New York: Plenum Press) p 143
33. Fackler J P Jr., Cotton F A and Barnum D W 1963 *Inorg. Chem.* **2** 97
34. Rosenwaks Y, Burstein L, Shapira, Yoram and Huppert D 1990 *J. Phys. Chem.* **94** 6842
35. Benjamin D and Huppert D 1988 *J. Phys. Chem.* **92** 4676
36. Ramsden J J and Grätzel M 1984 *J. Chem. Soc., Faraday Trans. 1* **80** 919
37. Kamat P V, Dimitrievic N M and Fessenden R W 1987 *J. Phys. Chem.* **91** 396
38. Grayson M 1984 *Encyclopedia of semiconductor technology* (NY: John Wiley & Sons)